remote sensing

MDPI

Article

WLQRP: A Weighting Link-Quality-Based Routing Protocol for Underwater Sensor Networks

Jianmin Yang [1,2,3], Jiahui Wang [1], Haitao Yu [4,*], Yexin Gao [1], Zhuoqian Wu [1] and Zhihong Peng [1]

[1] School of Ocean Engineering and Technology, Sun Yat-sen University, Zhuhai 519000, China; yangjm33@mail.sysu.edu.cn (J.Y.); wangjh333@mail2.sysu.edu.cn (J.W.); gaoyx39@mail2.sysu.edu.cn (Y.G.); wuzhq39@mail2.sysu.edu.cn (Z.W.); pengzhh25@mail2.sysu.edu.cn (Z.P.)
[2] Key Laboratory of Comprehensive Observation of Polar Environment (Sun Yat-sen University), Ministry of Education, Zhuhai 519082, China
[3] Southern Marine Science and Engineering Guangdong Laboratory (Zhuhai), Zhuhai 519000, China
[4] College of Tourism and Landscape Architecture, Guilin University of Technology, Guilin 541006, China
* Correspondence: albertyht@glut.edu.cn

Abstract: Due to challenges posed by long propagation distances, high mobility, limited bandwidth, multipath propagation, and Doppler effects in underwater acoustic sensor networks (UASNs), the design of routing protocols faces numerous complexities. To enhance reliability in sparse node regions and reduce network energy consumption, this paper proposes a dependable and energy-efficient routing protocol termed WLQRP for weighting link-quality-based routing protocol. WLQRP leverages link quality information between nodes for data forwarding. When computing the link quality between nodes, it considers not only the historical transmission success ratio between nodes and their immediate relay but also incorporates the link quality between the relay and the relay's next-hop nodes. This approach effectively reduces the likelihood of encountering void regions. Moreover, the protocol judiciously selects the next-hop node to improve transmission success rates, thereby minimizing data packet retransmissions and reducing energy consumption. We conduct MATLAB simulations to evaluate the WLQRP protocol, comparing it against the VBF (vector-based forwarding) and the HH-VBF (hop-by-hop vector-based forwarding) underwater routing protocol. Experimental results demonstrate that WLQRP enhances network performance in terms of data transmission rate, energy consumption, and end-to-end delay. These findings validate the efficacy of the proposed protocol.

Keywords: underwater sensor network; routing protocol; channel-aware communications

Citation: Yang, J.; Wang, J.; Yu, H.; Gao, Y.; Wu, Z.; Peng, Z. WLQRP: A Weighting Link-Quality-Based Routing Protocol for Underwater Sensor Networks. *Remote Sens.* **2023**, *15*, 5651. https://doi.org/10.3390/rs15245651

Academic Editor: Andrzej Stateczny

Received: 5 October 2023
Revised: 4 December 2023
Accepted: 5 December 2023
Published: 6 December 2023

Correction Statement: This article has been republished with a minor change. The change does not affect the scientific content of the article and further details are available within the backmatter of the website version of this article.

1. Introduction

The ocean has an abundance of fuel, minerals, and biological resources, and it is a main channel for global transportation [1]. The oceans hold vast reserves of fuel, minerals, and biological resources, serving as a vital global transportation route. Over the past century, nations have progressively increased their investments in oceanic research. As oceanic development accelerates, the need for underwater communication becomes increasingly urgent. The underwater environment has become a focus of significant attention due to advancements in sensing technology, leading to the emergence of underwater wireless sensor networks (UWSNs) as a promising option for exploration. Underwater wireless sensor networks (UWSNs) constitute a critical component of underwater communication technology, playing a pivotal role in underwater monitoring, development, and defense applications [2,3].

Unlike terrestrial wireless sensor networks (WSNs), UWSNs employ acoustic signals rather than radio frequencies for wireless communication. However, UWSNs face several inherent limitations, including prolonged and variable delays, narrow bandwidth, slow

signal decay, elevated error rates, and substantial noise [4,5]. Consequently, link quality assumes paramount importance when forwarding messages to the sink node. The majority of sensor nodes are battery-powered, rendering them challenging to replace or recharge once deployed underwater. Therefore, energy efficiency ranks as a primary concern when designing routing protocols tasked with collecting sensor data and routing it to the sink node. Moreover, UWSN sensor nodes drift with hydrodynamics, necessitating the consideration of network dynamics stemming from topological fluctuations.

In response to these challenges, this paper seeks to introduce a location-independent and energy-efficient routing protocol, wherein data packets are forwarded hop-by-hop from source sensor nodes to the sink node. The underwater acoustic communication routing protocol mainly solves the problem of data transmission between multiple nodes. The topology structure of the network, the period of data generation, the direction of data flow, and the flexibility of node deployment all affect the design of the routing protocol. In the past, two routing strategies have been presented: deterministic routing and opportunistic routing. In deterministic routing, if the network conditions do not change over time, the sender always selects the same node as the best next-hop node. In opportunistic routing, even if the network conditions do not change over time, the sender can choose different nodes as the optimal next-hop node [6–8]. Due to the unpredictability of link quality in underwater environments compared to changes in terrestrial radio links, opportunistic routing protocols can better handle changing network dynamics than deterministic routing schemes and are more suitable for networks in dynamic underwater environments [9]. The opportunistic routing protocol we propose leverages channel awareness and is designated as the weighting link-quality-based routing protocol (WLQRP).

In contrast to conventional routing protocols, which predominantly focus on selecting the next-hop node when choosing relay nodes, WLQRP attaches greater significance to link quality's influence. WLQRP scrutinizes historical transmission success records among nodes, encompassing not only the past transmission success rate between nodes and their immediate next-hop nodes but also factoring in link quality to subsequent next-hop nodes. This comprehensive channel quality evaluation during data packet transmission culminates in selecting the optimal hop for each data packet. Consequently, WLQRP enhances relay node selection efficiency, elevates data packet transmission success rates, curtails packet retransmissions, and diminishes energy consumption. Furthermore, WLQRP can harness topological information to circumvent connectivity gaps and shadow regions during routing, effectively minimizing the likelihood of encountering voids. To assess WLQRP's performance, simulations were conducted employing MATLAB. The outcomes indicate that our protocol excels in data packet transmission success rates, end-to-end delay, and latency. When juxtaposed with the vector-based forwarding (VBF) protocol and the HH-VBF (hop-by-hop vector-based forwarding), the experimental results manifest WLQRP's superiority in packet loss rates, energy consumption, delay, path selection, and various other aspects.

The rest of this paper is organized as follows. Section 2 summarizes previous work on underwater wireless sensor networks. In Section 3, we model the network. Section 4 describes the channel-aware routing protocol in detail. The simulation results on the MATLAB platform are explained in Section 5. At the end, the paper is summarized.

2. Related Works

Starting with this section, we provide an overview of the research performed on routing protocols in USANs. This includes a comprehensive analysis of their strengths, weaknesses, and challenges. It then introduces the WLQRP proposed in this article.

In UASN, routing protocols can be divided into three-dimensional location-based routing, depth-based routing, and location-free routing. Three-dimensional position-based protocols include VBF, HH-VBF, AHH-VBF, DFR, FBR, etc. Depth-based routing protocols include DBR, FDBR, VAPR, EEDBR, and Hydro Cast. Location-free routing is divided into cluster routing and beacon routing.

The VBF (vector-based forwarding) protocol [10] utilizes the geographic location information of each node to create a virtual pipeline between the source node and the sink node, and the nodes within or closer to the pipeline are more likely to be selected as the next node. However, when the number of nodes in the pipeline is small, the success rate of packet transmission of this routing protocol will be greatly reduced. The energy of nodes within the pipeline will be more easily consumed, which leads to an uneven energy distribution of nodes throughout the submarine network. The HH-VBF (hop-by-hop vector-based forwarding) protocol [11] and AHH-VBF (adaptive hop-by-hop vector-based forwarding) protocol [12], on the other hand, create virtual pipes at each hop to solve the problem of low transmission success rate at low node density. However, when the node density is higher, energy will be wasted excessively, and the data will have more conflicts. With the local topology information, The ACGSOR protocol [13] segmentation scheme divides the end-to-end path into several short opportunistic routing segments. Furthermore, a cooperation mechanism is applied to switch the transmission mode adaptively. However, the protocol consumes more energy. Xinbin Li et al. [14] propose an adaptive multi-zone geographic routing protocol (AMGR) that dynamically adjusts the neighbor information acquisition interval according to the topology change speed. In ref. [15], The underwater network is first divided into small cube spaces; thus, the data packets are supposed to be collaboratively transmitted by unit of small cubes logically.

Shin et al. studied a different flood-based geographic solution using their directional flooding-based routing (DFR) protocol [16]. In this protocol, each node broadcasts packets to all its neighboring nodes. The decision of whether to forward the packet is based on the BASE_ANGLE, which represents the direction from the sender S to the forwarding party F and the destination party D (the receiver). This decision is made by comparing the BASE_ANGLE to the reference angle included in the package. The change in the underwater channel is addressed by gradually adjusting the reference angle based on the link quality. A smaller flooding area is achieved with a better reference angle. Since obtaining accurate underwater geographic information can be challenging or costly, some protocols make use of partial geographic information. Focused beam routing (FBR) [17] is based on the concept of multiple sensors and multiple channels, using multiple acoustic sources, receivers, and focused beamformers for data transmission. FBR can improve transmission distance and signal quality by focusing acoustic energy in a specific direction, overcoming water absorption and scattering problems. Multiple data streams can be transmitted simultaneously, increasing the data transmission rate and throughput. However, it also has problems in terms of high hardware requirements, diffusion overlap due to the multipath effect, and energy consumption. In [18], Quansheng Guan et al. propose a distance-vector-based opportunistic routing (DVOR) scheme to address void and detouring.

Yan, H. et al. [19] proposed a depth-based routing protocol with a greedy algorithm, DBR (depth-based routing), which differs from other protocols in that it does not need to use specific geographic location information. Instead, it uses depth as a factor for selecting the next hop node and only requires depth information. This protocol avoids the need for complex location techniques. The transmission of data is limited to a one-way flow, from the lower level to the higher level. This routing protocol selects the next node based on whether it is closer to the surface of the sea than the node at this point, and if the packet is closer to the sea, it will be transmitted to that specific node. On this basis, Mohammadi, R. et al. [20] proposed an improved protocol, FDBR (fuzzy depth-based routing), which not only utilizes depth information but also takes hop count and energy information into account more comprehensively. This leads to enhanced network energy usage and improved delay performance. In order to reduce the probability of encountering void holes in the sparse networks, Haitao Yu et al. [21] presented a weighting depth and forwarding area division DBR routing protocol called WDFAD-DBR. Noh Y. et al. [22] proposed VAPR (void-aware pressure routing), a void-aware pressure routing protocol, which utilizes the sequence number, hop number, and depth information to enable the selection of the next hop node closest to the surface receiver, thereby selecting the shortest data transmission path and

maintaining a high packet transmission rate even in the presence of voids. In order to extend the life cycle of the network and balance the energy consumption, EEDBR [23] considers two indexes, depth and remaining energy, when forwarding packets. When a node receives a packet, it calculates the retention time based on its remaining energy and position in the forwarding list. In ref. [24], Lee et al. proposed pressure routing (hydro cast) for underwater sensor networks. The next hop node is selected in a similar way to DBR, but it adopts an anti-gap mechanism and limits co-channel interference to improve network performance. Ashraf, S. et al. [25] proposed a confined energy depletion (CED) opportunistic routing (OR) mechanism in which the depth factor of the compute node is used to further narrow the selection range of the next-hop trunks. In ref. [26], a geographic and cooperative opportunistic routing protocol (GCORP) is proposed. In the GCORP protocol, initially, a multiple sink-based network architecture is established. Then, a relay forwarding set is determined by the source node on the basis of the depth fitness factor. Bouk SH et al. [27] proposed the energy and depth variance-based opportunistic void avoidance (EDOVE) scheme to gain energy balancing and void avoidance in the network. EDOVE considers not only the depth parameter, but also the normalized residual energy of the one-hop nodes and the normalized depth variance of the second hop neighbors.

The H2-DAB (hop-by-hop hop dynamic addressing based) protocol proposed by AYAZ M et al. [28] does not even need to use any location information. In this protocol, the surface receiver first broadcasts a hello packet to the submarine nodes, and all the nodes receive it and obtain hop count information from that node to the receiver. In the subsequent packet transmission, the forwarding of the next node is determined solely by the hop count information. Wenbo Zhang et al. [29] designed a Nonuniform clustering (NC) algorithm in which clusters are generated according to different node densities. The simulation results show that compared with the classical routing algorithm, the proposed algorithm has a higher transmission efficiency, requires less energy consumption, and can more effectively extend the network's lifetime. In ref. [30], the whole network model is regarded as a 3D cube from the grid point of view, and this 3D cube is divided into many small cubes, where a cube is seen as a cluster. The proposed protocol shapes an energy consumption model considering the residual energy and location of sensor nodes to select the optimal cluster-heads. Zhiping Wan et al. [31] proposed the ACUN protocol. The algorithm uses a multi-level hierarchical network structure based on the distance between cluster heads and the sink node and the residual energy of a cluster head to determine the size of the competition radius. In ref. [32], the authors propose a multi-layer cluster-based UWSN energy saving (MLCEE) protocol to solve the problem of hotspots and energy consumption. MLCEE first divides the entire network into layers and then clusters nodes in the same layer. Finally, the cluster head (CH) selects the next hop in the CH based on the larger fitness value, the smaller hopid, and the smaller number of layers.

Stefano Basagni et al. [33] proposed CARP, which utilizes link quality, avoids loops, and bypasses nulls through a simple topology. This network improves packet delivery and saves energy; but again, at the cost of higher latency. In [34], ZhangBing Zhou et al. introduced E-CARP, an enhanced iteration of the channel-aware routing protocol (CARP) initially developed by S. Basagni et al. E-CARP allows sensing data to be cached at sink nodes to prevent these packets from being forwarded across the network, reducing data retransmission. Furthermore, by enhancing the technique for selecting relay nodes in CARP, the selected relay nodes are given a higher reuse priority, which reduces the communication cost and improves the network performance to a great extent.

Compared with the above-mentioned related works, two prominent advantages of WLQRP are summarized as follows:

1. WLQRP scrutinizes historical transmission success records among nodes, encompassing not only the past transmission success rate between nodes and their immediate next-hop nodes but also factoring in link quality to subsequent next-hop nodes. This comprehensive channel quality evaluation during data packet transmission culminates in selecting the optimal hop for each data packet. Consequently, WLQRP

enhances relay node selection efficiency, elevates data packet transmission success rates, curtails packet retransmissions, and diminishes energy consumption.
2. WLQRP takes the energy of the next-hop node into the calculation of link quality, which can effectively balance the energy consumption between nodes and extend the lifetime of the network.
3. WLQRP can harness topological information to circumvent connectivity gaps and shadow regions during routing, effectively minimizing the likelihood of encountering voids.

3. System Model

The focus of this article is the 3D underwater acoustic sensor network model, which is described in this section. Furthermore, we present the energy model and the acoustic propagation model, which act as the theoretical foundation for our proposed routing protocol.

3.1. Network Architecture

The suggested protocol utilizes a single-sink design, which includes anchored nodes, relay nodes, and one central sink node. The sink node, labeled as A, is located in the middle of the water surface. Meanwhile, N sensor nodes are evenly spread throughout a three-dimensional underwater area in the form of a cubic shape, as shown in Figure 1. Anchored nodes are securely positioned at the bottom of the ocean and are responsible for sensing and collecting data. Relay nodes are deployed at various depths and have the role of finding paths toward the destination, forwarding received packets to the next hop and sometimes collecting environmental data. The sink node functions as the endpoint for routing and is equipped with both underwater acoustic and above-water radio modems. Underwater communication is achieved through the acoustic link, while communication above the water surface is enabled through the radio link. Anchored nodes detect data and send them to the sink node on the water surface through intermediary nodes. Then, the sink node employs the radio link to transmit the received data to a satellite, which in turn relays the data to the control center located on the shore.

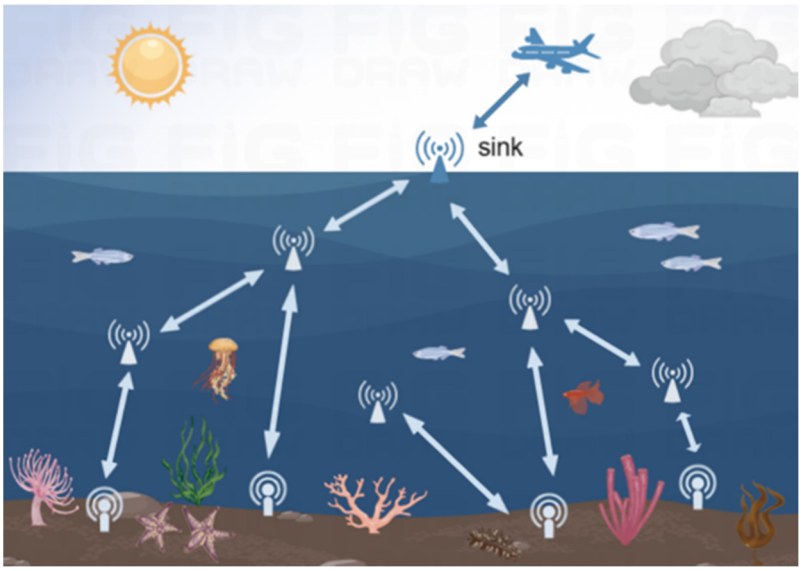

Figure 1. Network architecture.

In this study, the following assumptions are made:

1. The surface sink node has an unlimited energy supply;
2. Each underwater sensor node can determine its location as well as the sink node's location on the water surface using location services.
3. Sensor nodes consistently have data to transmit, and data collection follows a periodic mechanism;

4. The sink node acts as a superior node capable of receiving multiple packets simultaneously without any collisions.

These assumptions lay the foundation for the proposed protocol and the subsequent analysis.

3.2. Energy Consumption Model

There are two types of losses that occur with underwater acoustic signals: absorption loss and spreading loss. These losses are affected by different factors, including signal frequency, transmission distance, and bandwidth. In this article, the Thorp propagation model is employed to create the underwater acoustic channel for the energy consumption model [35]. To calculate the total loss of an underwater acoustic signal with a frequency of 'f' in kHz at a distance of 'd' in km, the following formula is used:

$$A(d, f) = d^k \alpha(f)^d \tag{1}$$

where 'k' represents the energy spreading factor and $\alpha(f)$ denotes the absorption coefficient. The energy spreading factor, 'k', describes the propagation geometry, taking a value of 1 for cylindrical spreading, 1.5 for practical spreading, and 2 for spherical spreading. In this case, we set 'k' to 1.5. The absorption coefficient $\alpha(f)$ can be determined using Thorp's formula shown in Equation (2), measured in dB/km:

$$10 \log \alpha(f) = \frac{0.11 f^2}{1 + f^2} + \frac{44 f^2}{4100 + f^2} \tag{2}$$

Equation (2) can be used for frequencies above 400 Hz. Equation (3) can be used to calculate the absorption coefficient of a signal at frequencies below 400 Hz [36]:

$$10 \log \alpha(f) = 0.002 + \frac{0.11 f^2}{1 + f^2} + 0.011 f^2 \tag{3}$$

The expression for the energy consumed by the nodes to transmit a packet containing 'm' bits over a distance 'd' is given by [37]:

$$E_{tx}(m, d) = m E_{elec} + m T_b C H d e^{\alpha(f) d} \tag{4}$$

where E_{elec} is the unit energy consumed by the electronics to process one bit of message, T_b refers to the bit duration, C is equal to $2\pi(0.67)10^{-9.5}$, and H represents the depth of node.

The energy consumption of a sensor node when receiving m bit E_{rx} can be obtained by:

$$E_{rx}(m, d) = m E_{elec} \tag{5}$$

the residual energy E_{rx} of a sensor node can calculated as:

$$E_{resi} = E_{init} - (E_{rx} + E_{tx}) \tag{6}$$

3.3. Acoustic Propagation Model

The temperature, pressure, and salinity of seawater dictate the speed at which sound travels in underwater environments. This relationship can be expressed as a function that incorporates the following variables [38]:

$$\begin{aligned} c = 1448.96 + 4.519T - 5.304 \times 10^{-2} T^2 + 2.374 \times 10^{-2} T^3 + 1.304(S - 35) + 1.63 \times 10^{-1} D \\ + 1.675 \times 10^{-7} D^2 - 1.025 \times 10^{-2} T(S - 35) - 7.139 \times 10^{-13} T D^3 \end{aligned} \tag{7}$$

The propagation speed of sound in meters per second is represented by 'c'; the temperature, measured in degrees Celsius, is denoted by 'T'; the salinity, measured in parts per thousand, is represented by 'S'; and the depth, in meters, is denoted by 'D'. It is important to mention that the speed of sound increases with higher values of temperature,

depth, and salinity. Equation (7) is applicable if the conditions are satisfied as follows: $0 \leq T \leq 30,\ 30 \leq S \leq 40,\ \ 0 \leq D \leq 8000$.

4. Protocol Description

The network initialization process is defined first, followed by a detailed explanation of data forwarding.

The network initialization is achieved by the sink broadcasting Hello packets, and the nodes gradually establish connectivity through the process of updating their hop counts and retransmitting data packets upon receiving the Hello packets. A detailed description of this process is provided in Section 4.1. Figure 2 shows a flowchart for the network initialization process.

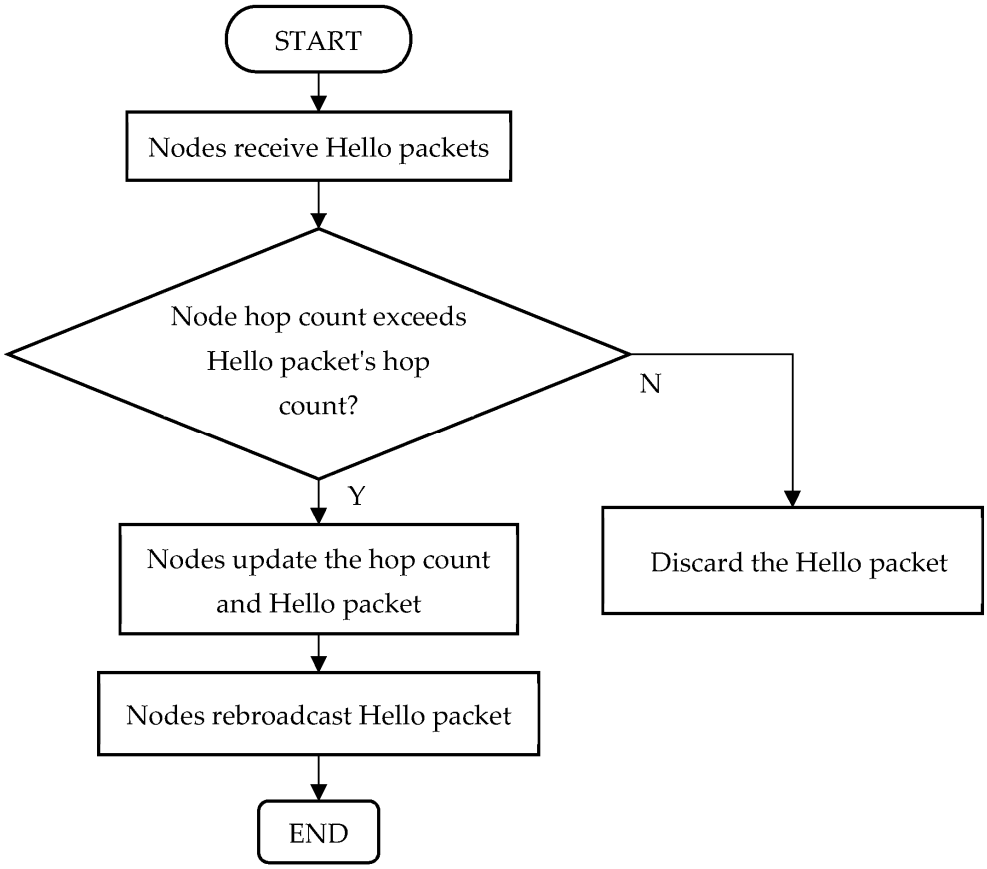

Figure 2. Flowchart for network initialization process.

Following the successful initialization of the network, the data forwarding process commences with a preliminary handshake phase. Assuming node x is tasked with data forwarding, the initial step entails engaging in a handshake with its adjacent nodes. Node x initiates the process by dispatching HANDSHAKE-S packets to its neighboring counterparts. Upon receipt of these packets, the neighboring nodes respond by generating HANDSHAKE-R packets, which are then transmitted back to node x.

Subsequently, the completion of the handshake phase between node x and its neighboring nodes is realized. A detailed description of this process can be found in Section 4.2. A visual representation of the handshake phase is presented in Figures 3 and 4. Figure 3 shows the process of sending HANDSHAKE-S and receiving HANDSHAKE-R when a node needs to forward data, and Figure 4 shows the process by which a neighbor node receives HANDSHAKE-S and sends HANDSHAKE-S.

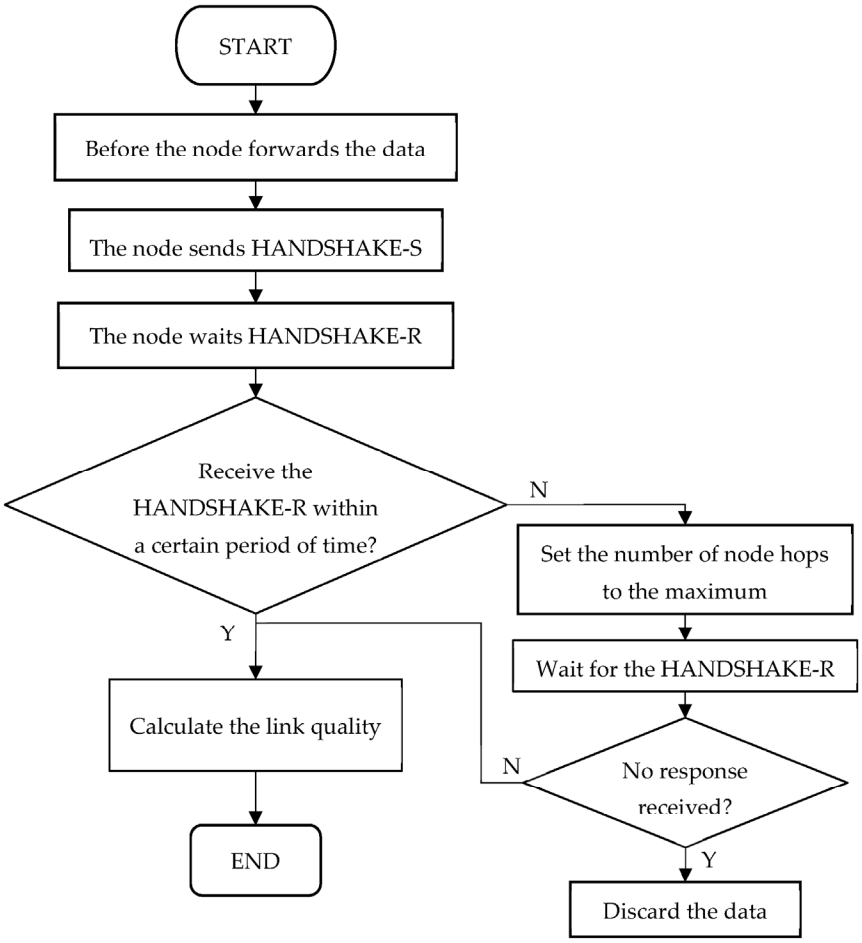

Figure 3. Flowchart for the node.

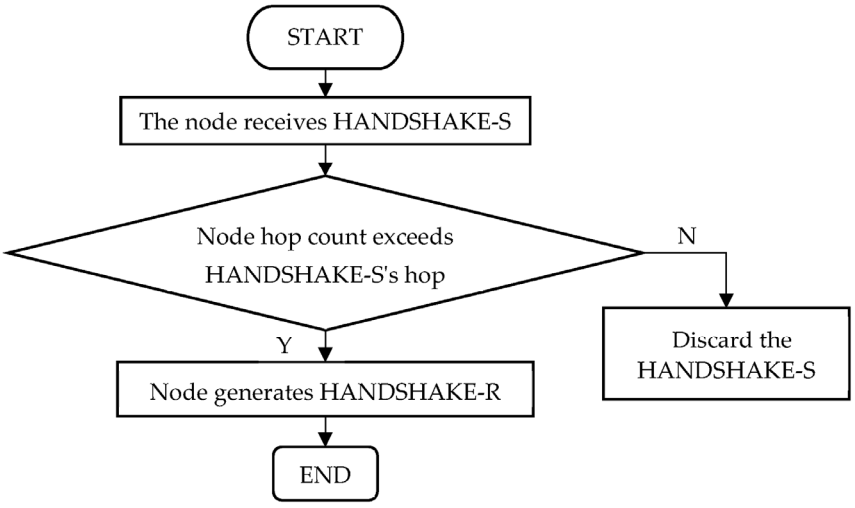

Figure 4. Flowchart for the neighbor node.

The subsequent phase of data forwarding unfolds with the execution of the data transmission process. Upon reception of HANDSHAKE-R packets from its neighbors, node x computes the link quality metric with each neighboring node using the prescribed Equation (8). Subsequently, node x selects the neighbor with the highest computed link quality to facilitate data transmission. Acknowledgment (ACK) packets are relayed back to node x by the recipients of the transmitted data. It is crucial to emphasize that only those

neighbors whose link quality surpasses a designated threshold can successfully receive data packets. In instances where all neighbors possess link quality values beneath the threshold, the node temporarily stores the packet in a cache queue for the next send. Additionally, in cases where node x fails to receive ACK packets and retransmission, it proceeds to select the neighbor with the second-highest link quality for data forwarding, and this iterative process continues accordingly. Section 4.3 provides a detailed description of this process. The procedural depiction of the data forwarding phase is graphically presented in Figure 5.

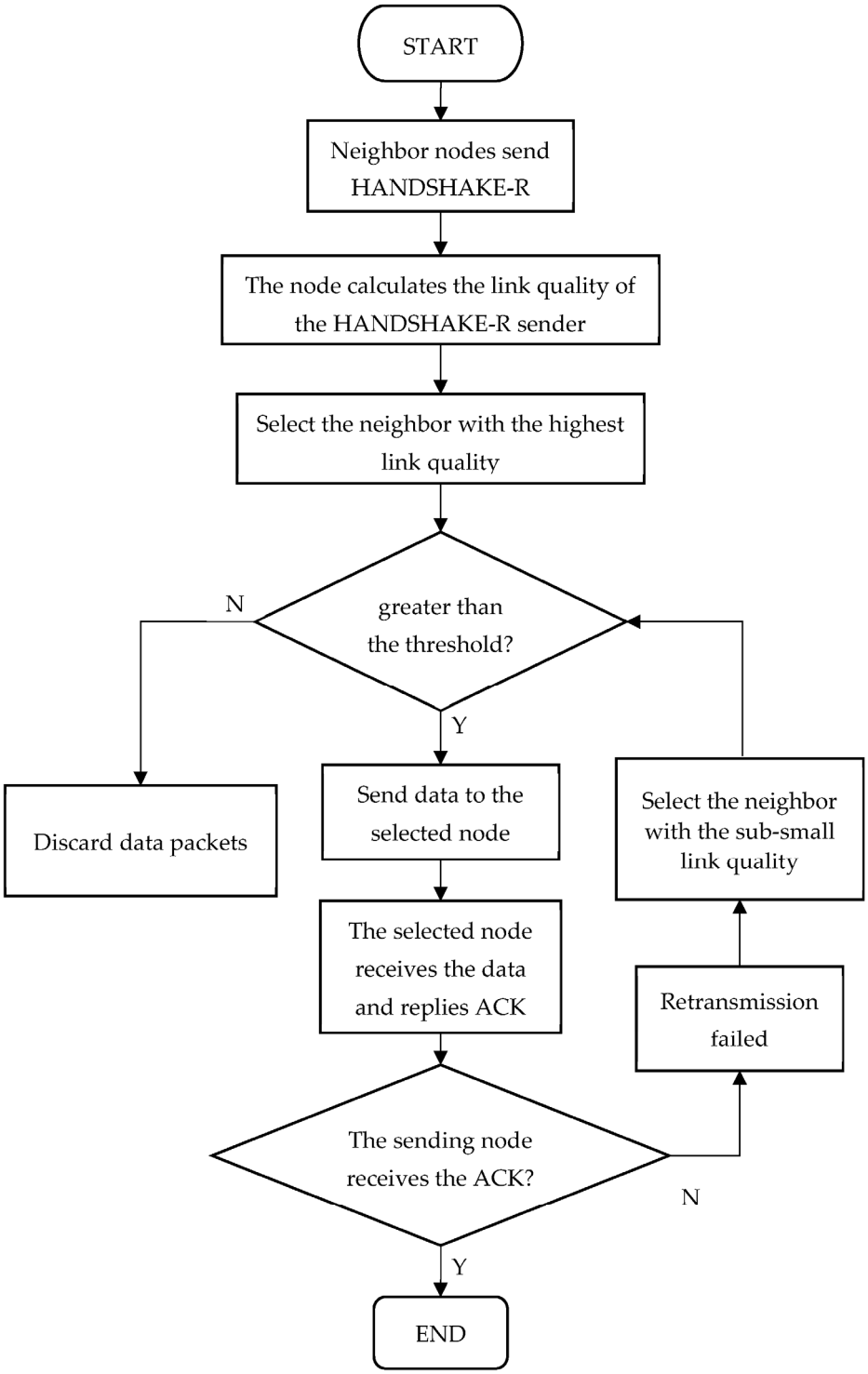

Figure 5. Flowchart for the data forwarding phase.

4.1. Network Initialization and Hop Count Setting

At the commencement of network initialization, the sink node initiates a regular and periodic dissemination of Hello packets across the entire network, adhering to a consistent time interval. The Hello packet format is (forwarding node, hc), including the ID of the forwarding node (initially the sink ID) and the hop count (initiated to 0). Upon receiving a Hello packet, the recipient node (referred to as node x) conducts a comprehensive assessment. It meticulously checks whether its current hop count variable HC(x) exceeds the hop count hc carried by the received Hello packet. If this condition is met, node x proceeds to update its hop count HC(x) by incorporating the value contained within the Hello packet plus 1. Subsequently, it retransmits the Hello packet, ensuring that the propagated packet carries the newly updated hop count HC(x) and forwarding node updates to x. Conversely, in the event that the condition is not satisfied, node x responsibly discards the received Hello packet, thereby preserving the integrity and consistency of the hop count. The above-mentioned process is repeated until the Hello packet goes through all the reachable sensors. A description of the hop count setting algorithm is shown below as Algorithm 1. Upon the culmination of this setup stage, each node within the network acquires precise and up-to-date information pertaining to its hop distance to the sink node.

Algorithm 1. Algorithm for hop count setting

```
Sensor nodes N = {1, 2, x, y, . . ., n} with their hop count HC
The hop count of the sink is initiated to 0, and other nodes is initiated to infinity
Surface sink broadcasts a Hello packet (forwarding node, hc)
if node x receives a Hello packet then
   Compare the node hop count HC(x) and the Hello packet carrying hop count
   if HC(x) > hc then
      HC(x)←hc + 1
      Rebroadcast the Hello packet by setting hc←HC(x) and forwarding node←x
   else
      Discard the Hello packet
   End
end
```

4.2. Handshake Phase

During the handshake phase, two types of packets are employed: HANDSHAKE-S and HANDSHAKE-R. HANDSHAKE-S, sent by the initiating node, follows the format (TypeID, NodeID, PacketID, HC, Q-packet). TypeID designates the packet type, NodeID embodies the node ID of the HANDSHAKE-S sender, PacketID stands for HANDSHAKE-S ID (distinct for each request-initiating packet), HC indicates the hop count value of the HANDSHAKE-S sender, and Q-packet constitutes a data packet queue. This queue includes pending forwarding data represented by (pktsrc, pktid) pairs, where pktsrc represents the source node ID and pktid is the data packet ID.

HANDSHAKE-R serves as the response packet sent by a node upon receiving HANDSHAKE-S, having the format (TypeID, NodeID, PacketID, HC, Packet-Bit, Energy, Link-Quality). TypeID denotes the packet type, NodeID designates the node ID of HANDSHAKE-R sender, PacketID signifies the received HANDSHAKE-S ID, HC indicates the hop count value of the HANDSHAKE-R sender, and Packet-Bit indicates whether node y holds pending forwarding data in its cache, with the corresponding queue bit set to 1 if data are present. Energy denotes the energy of the HANDSHAKE-R sender, and Link-Quality quantifies the link quality between two nodes engaged in the handshake, computed as detailed below.

Prior to the initiation of data transmission between nodes, a handshake phase is initiated. When node x possesses one or more packets intended for forwarding, it proceeds to broadcast HANDSHAKE-S packets. In the event that a HANDSHAKE-R response is not received from neighboring nodes within the specified time window, the hop count of the node is subsequently adjusted to its maximal value. Subsequently, an additional temporal

interval is observed. Should a response fail to be received even during this extended period, the node proceeds to effectuate the discarding of the data packet.

Upon receiving the HANDSHAKE-S packet from node x, node y conducts a hop count comparison between the two nodes. If HC(x) is greater than the node y's hop count, node y checks its own cache queue for the presence of data packets included in the Q-packet. If such data packets are found, the corresponding bit is set to 1, following which node y generates a HANDSHAKE-R packet and sends it back to node x. However, if HC(x) is less than the node y's, node y simply discards the received HANDSHAKE-S packet. The pseudocode for the procedure is given in Algorithm 2.

Algorithm 2. Upon receiving HANDSHAKE-S from node x

```
After node y receives the HANDSHAKE-S packet from node x
Compare the hops of nodes x and y
if HC(x) < HC(y) then
   drop HANDSHAKE-S
else
   node y checks its own cache queue for data packets included in the Q-packet
   if node y has already received packet in Q-packet then
      Set packet position in Packet-Bit to 1
      Calculate Link-Quality
      Send HANDSHAKE-R = (TypeID, NodeID, PacketID, HC, Packet-Bit,
            Energy, Link-Quality)
   end
end
```

4.3. Selecting the Optimal Relay and Data Forwarding

Following the reception of HANDSHAKE-R responses from neighbor nodes, the node proceeds to identify the most suitable intermediary relay. Subsequently, leveraging the Packet-Bit information derived from the chosen relay node's HANDSHAKE-R response, node x determines which data packets within the pending forwarding queue can be pruned prior to forwarding the remaining packets to the selected relay node. Algorithm 3 summarizes the processing details upon receiving HANDSHAKE-R.

During the process of selecting the optimal relay, the primary criterion involves evaluating the link quality of the neighboring nodes that have responded. In a scenario where a data packet is delivered to node x, encompassing a set of m neighboring nodes including y, the criterion for x's next-hop node selection involves identifying the neighbor with the most robust link quality that surpasses a pre-established threshold. The computation of link quality for neighboring nodes adheres to the subsequent formula:

$$lq_{x,y} = \alpha\left[\beta S_{x,y} + (1-\beta)\frac{1}{HC(y)}\right] + (1-\alpha)\left[\gamma\overline{lq_{y,N}} + (1-\gamma)lq_{y,N\_}m\right] + \delta E(y) \quad (8)$$

$S_{x,y}$ represents the transmission success rate between nodes x and y, where the success rate is calculated as the ratio of actual data forwarding times to theoretical data forwarding times. Theoretical data forwarding times pertain to situations where nodes x and y achieve successful handshakes and designate y as the subsequent hop for data relay. Actual data forwarding times entails the successful transmission of data from node x to node y following a successful handshake. In other words, if the subsequent relay is selected as y but x fails to forward packets to y, then the transmission success rate will be reduced. Upon the determination of the subsequent hop node, the heterogeneity in link quality introduces variability in the consistent success of data packet transmissions. Therefore, the probability of successful data packet transmission serves as an indicator of channel quality, thereby aiding the WLQRP protocol in selecting relay nodes situated within favorable communication channels.

Algorithm 3. Upon receiving HANDSHAKE-R

After node x receives the HANDSHAKE-R packet from neighbors
Select all neighbor nodes that have replied to HANDSHAKE-S sent by x
Calculate all neighbors' link quality
Select the neighbor node with the highest link quality
if the highest link quality greater than threshold **then**
  Node x checks Packet-Bit in received HANDSHAKE-R
  Remove duplicate data packets
  Send data packets
else
  The node temporarily stores the packet in a cache queue for the next send.
end
if y has received data packets **then**
  node y sends ACK
end
if x has received ACK **then**
  Packets are transmitted successfully
else
  x retransmits data packets (up to three times)
  if x has received ACK **then**
    Packets are transmitted successfully
  else
    Node x selects another relay to transmit data packets
  end
end

$\overline{lq_{y,N}}$ denotes the average link quality between node y and its neighboring nodes (except node x), while $lq_{y,N\_}m$ signifies the maximum link quality value among all of y's neighboring nodes. By incorporating the average and maximum values of link quality among neighboring nodes for the subsequent hop, WLQRP is adept at skillfully circumventing link vulnerabilities and thereby mitigating the risk of encountering routing traps. $E(y)$ represents the energy level of node y, thus mitigating the risk of data packet loss arising from inadequate energy resources within node y.

The constants $\alpha, \beta, \gamma, \delta$ in the formula are adjustable parameters, allowing for manipulation of the weighting between link quality and node energy pertaining to subsequent and subsequent-to-subsequent hop nodes. In scenarios characterized by suboptimal link quality, elevating the weighting of subsequent-to-subsequent hop link quality ensures the protocol's reliability.

As shown in Figure 6, node S is the forwarding node, and node A, node B, and node R are neighbors of node S. When node S needs to send data, it first sends HANDSHAKE-S. After neighbor nodes A, B, and R receive HANDSHAKE-S, they first check whether their hop count is greater than the hop count carried in HANDSHAKE-S. As can be seen from the figure, node B has a larger number of hops than node S. Therefore, node B discards the HANDSHAKE-S, node A and node R send HANDSHAKE-R to node S, and node S selects the node with the highest link quality that is greater than the threshold from the nodes sending HANDSHAKE-R as the best relay. The link quality of the three is calculated to be 0.77 and 0.65, respectively. According to the forwarding policy of WLQRP, the node R with the link quality of 0.77 is selected as the next hop node. When calculating the link quality between node S and nodes B and R, not only the link situation between node S and node R is considered, but also the link situation between nodes R and their neighbors. This also demonstrates that only the link condition between the node and the next hop node is good enough to make the next hop node a relay node, and the neighbor status of the next hop node is also an important judgment basis. This can effectively avoid the route falling into a void.

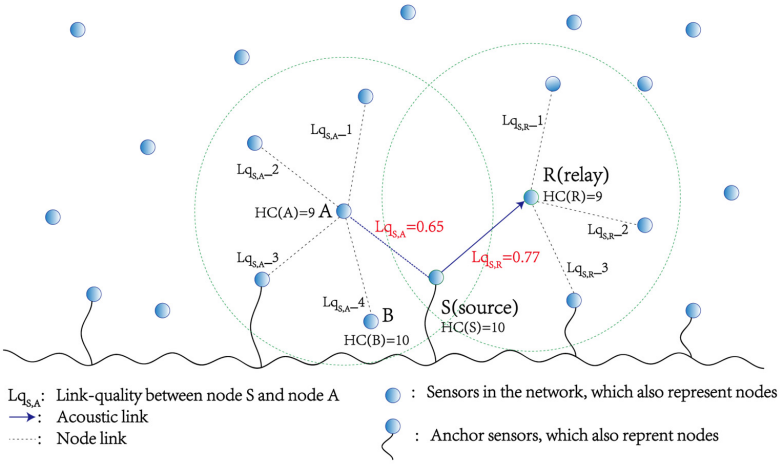

Figure 6. The data forwarding phase.

Once the optimal relay is determined, node x proceeds to forward a set of data to node y. Upon successful data reception, node y sends an acknowledgment (ACK) message back to node x. If node x does not receive an ACK confirmation from node y within the specified wait time (round-trip time of the data packet), x will resend the data. The maximum number of retransmissions is 3. If x does not receive the ACK packet after retransmission, it proceeds to select the second-highest link quality node for data transmission, and this process continues iteratively. If the link quality of all neighboring nodes of node x falls below a predefined threshold, the node temporarily stores the packet in a cache queue for the next send. Once the packet is successfully sent, it will be removed from the cache queue. If the cache is full, the packets are dropped one-by-one in a first-in, first-out order.

5. Simulation Results

5.1. Simulation Setup

In the simulation, data collection is performed by a single sink node positioned on the water surface, while all the nodes are randomly dispersed within a three-dimensional area measuring 10,000 × 10,000 × 10,000 m^3. These sensor nodes have an initial energy of 1000 J, a transmit power of 100 W, a receiving power of 8 W, and a power consumption of 2 mW for an idle state. During the simulation process, the simulation is conducted using a loop structure where the number of nodes increases from 300 to 600. Nodes located within 3000 m from the bottom are referred to as source nodes, and for each round of the network, a source node is randomly chosen to generate 100 packets for transmission. Each data packet has a size of 64 bytes, with an additional 8 bytes for the header. The primary simulation parameters are provided in Table 1. The above are the settings of the common parameters of the three protocols. In addition to this, regarding the VBF [10] and HH-VBF [11] protocols, the radius of the "routing pipe" is set to 2000, and the Tdelay is set to 0.1 s.

Table 1. Parameter settings.

Parameter	Value
Node numbers	300–600
Network dimensions (m^3)	10,000 × 10,000 × 10,000
Data packet size (bytes)	64
Header size of data packet (bytes)	8
Size of other packets (bytes)	8
Initial energy (J)	1000
Maximum transmission range (m)	2000
Transmission power (W)	100
Receiving power (W)	8
Transmission rate (kbps)	2

5.2. Metrics

Throughout the simulations, we utilize the proposed WLQRP methodology as a basis for comparison with VBF while employing the following performance metrics:

1. Packet loss ratio: The packet loss ratio is defined as the quotient of the number of packets received by the sink and the number of packets generated by the network.
2. Residual energy ratio: The average remaining energy of the node after the packet transmission is completed in the sensor network relative to the initial energy of the node is referred to as the energy ratio.
3. Consumed energy per packet: The definition of consumed energy per packet is the total energy consumed by the network to transmit packets divided by the number of packets received by the sink node.
4. End-to-end delay: End-to-end delay is the collective time it takes from when packets are initially sent from the source node to when they are successfully received by the sink node. This includes the time it takes for the packets to propagate, the time it takes for them to be transmitted, the time they spend being held, and the time spent on calculations.
5. Hop count: The hop count is the average hop count taken by a packet to travel from the source node to the receiving node in the shortest time in a simulation.
6. Deviation factor: The proportion of the disparity between the cumulative propagation distance and the direct distance (from source to sink node) to the direct distance from the source node to the sink node [12].

$$Deviation\ Factor = \frac{TotalDist - StraitLineDist}{StraitLineDist}$$

TotalDist denotes the aggregate propagation distance traversed by a successfully received packet from the source node to the sink node, while StraitLineDist represents the direct linear Euclidean distance between the source node and the sink node. The magnitude of the propagation deviation factor directly influences the extent of the incremental propagation distance. Consequently, the propagation deviation factor aptly characterizes the supplementary propagation overhead endured by the packet within the network. This additional overhead encompasses heightened latency and augmented energy consumption.

5.3. Results and Analysis

5.3.1. Packet Loss Ratio

Figure 7 depicts the packet loss ratio of the WLQRP, VBF, and HH-VBF protocols as the number of nodes increases. It can be inferred from the graph that the packet loss ratio of the WLQRP, VBF, and HH-VBF protocols decreases with the augmentation of node quantity. This phenomenon is attributed to the elevated likelihood of discovering available neighboring nodes by these protocols as node density escalates, thereby diminishing the probability of encountering voids resulting in packet loss. Additionally, the graph illustrates that under low node density conditions, WLQRP exhibits superior performance compared to VBF and HH-VBF. This performance advantage can be attributed to the relay selection mechanism of WLQRP, enabling it to identify dependable next-hop nodes even within sparsely connected node networks, thereby mitigating the packet loss ratio. As the network becomes denser, WLQRP's performance further improves, with the packet loss ratio potentially declining to less than 0.05%.

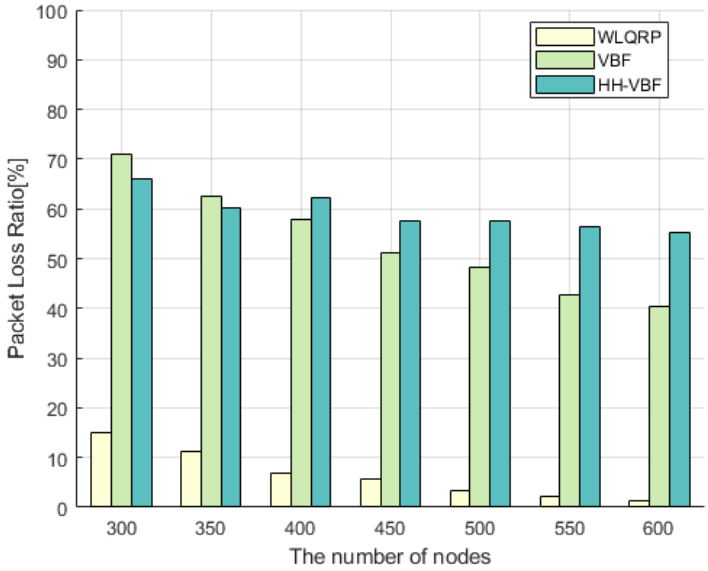

Figure 7. Packet loss ratio.

5.3.2. Hop Count

The presented graph illustrates the variation in hop counts that data packets undergo, from their generation to eventual reception at the sink node, as the number of nodes increases. It is evident from the graph that, with an escalation in the node count, the hop count in the WLQRP protocol demonstrates a steady decrease, in contrast to the VBF and HH-VBF protocols, where the hop count experiences an upward trend. This contrast emerges due to the employed VBF and HH-VBF network structure, which is akin to the multi-source node network configuration employed by WLQRP. In other words, the network includes multiple pipelines. The relay selection mechanism of VBF and HH-VBF involves selecting the neighbor node within the pipeline with the minimal anticipated factor as the optimal relay. This selection strategy results in an inability to effectively choose appropriately distanced next-hop nodes as the node density increases, leading to an increase in the hop count for packet forwarding to the sink node. In contrast, WLQRP's relay selection mechanism comprehensively accounts for distance factors of the next-hop node (i.e., the hop count to the sink node), enabling it to choose relay nodes as proximate to the sink node as feasible. Consequently, WLQRP excels in densely populated networks, effectively minimizing hop counts for packet forwarding (Figure 8).

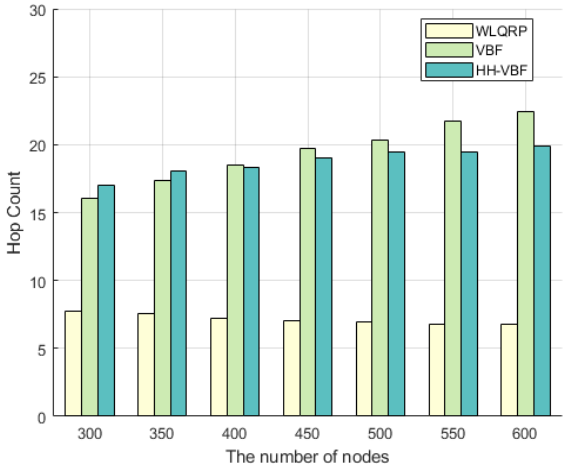

Figure 8. Hop count.

5.3.3. End-to-End Delay

Figure 9 presents the temporal variations in WLQRP, VBF, and HH-VBF as the node count increases. The graphical depiction indicates that WLQRP experiences a gradual reduction in latency as the node count grows. This trend is congruent with the observations in Figure 4, where WLQRP's hop count follows a comparable trajectory with respect to the node count. This congruence arises due to the strong positive correlation between packet hop count and latency. In the context of WLQRP, packet latency encompasses the transmission time within the channel and the duration expended at relay nodes for reception and subsequent forwarding. This implies that the time spent at relay nodes for reception and forwarding contributes significantly to the overall latency. Consequently, as the number of relay nodes traversed by the packet increases, the latency proportionately rises.

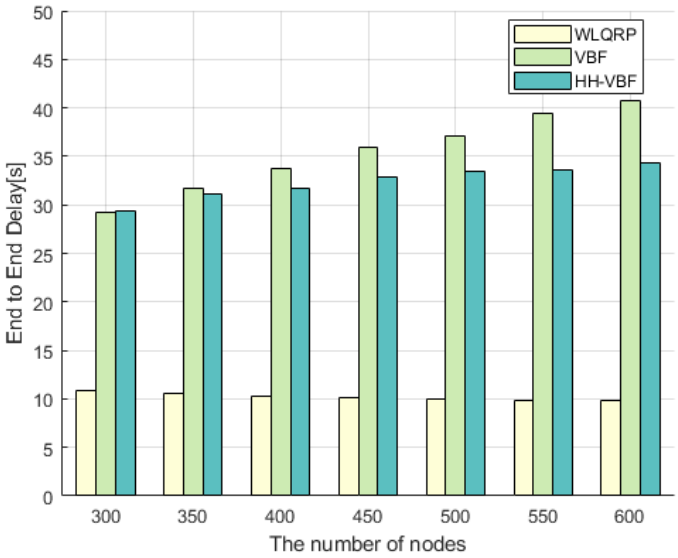

Figure 9. End-to-end delay.

Figure 8 reveals a decline in the packet hop count as the node count increases, and correspondingly, the latency of the packets decreases in line with node count escalation. The graph further suggests that WLQRP outperforms the VBF protocol and HH-VBF in terms of latency. One contributing factor to this phenomenon is that VBF and HH-VBF entail a waiting period during next-hop selection, thereby introducing a fraction of its latency. However, the substantial discrepancy in latency between the two routing protocols can be primarily attributed to WLQRP's lower average hop count compared to VBF. The reduction in relay transmission time achieved by the WLQRP protocol significantly diminishes latency, leading to a considerable reduction compared to VBF and HH-VBF.

5.3.4. Residual Energy Ratio

Figure 10 depicts the variations in the residual energy ratio of nodes for the three protocols as the number of nodes increases. The residual energy ratio of a node signifies the ratio between the average remaining energy of all the nodes, following the completion of data packet forwarding, to the initial energy level of the nodes in the network. As evident from the graph, an augmentation in node count results in a progressive increase in the residual energy ratio for WLQRP, whereas VBF and HH-VBF exhibit a corresponding decline. This phenomenon arises primarily due to energy consumption being dominated by data packet forwarding and reception, with forwarding constituting a substantial portion. With an increase in node count, the frequency of packet forwarding diminishes in WLQRP, thereby leading to a gradual rise in the residual energy ratio.

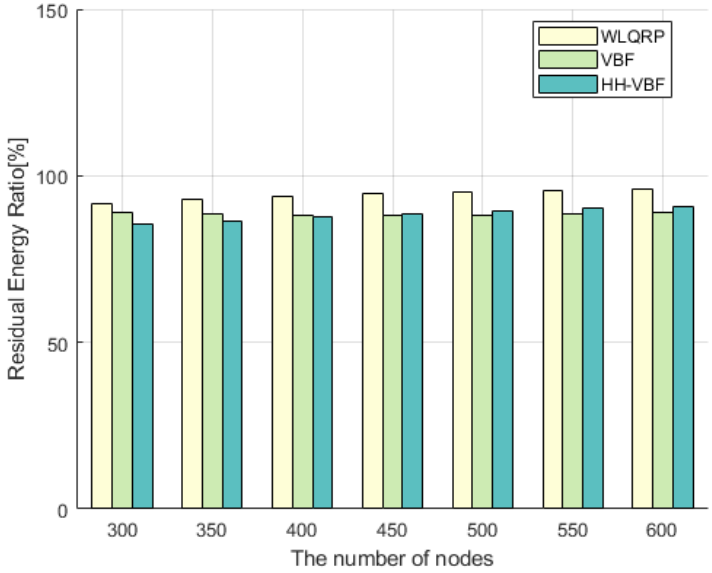

Figure 10. Residual energy ratio.

However, as inferred from preceding graphs, an elevation in node count for VBF corresponds to an increase in hop count, consequently resulting in a decrease in the residual energy ratio.

5.3.5. Consumed Energy per Packet

Figure 11 illustrates the contrast in average energy consumption of data packets between the two protocols as the number of nodes increases. Notably, the trend displayed in this graph is inverse to that observed in Figure 4. With an escalating node count, WLQRP demonstrates a progressive reduction in the average energy consumption of data packets, while VBF exhibits a corresponding increase. The energy consumption of HH-VBF is higher than that of VBF, which is reasonable because HH-VBF finds more paths, increasing energy consumption. As deduced previously, a higher number of packet transmissions leads to increased energy consumption. Consequently, considering the packet forwarding hop count, WLQRP experiences a decrease in the average energy consumption of data packets, whereas VBF encounters an increase.

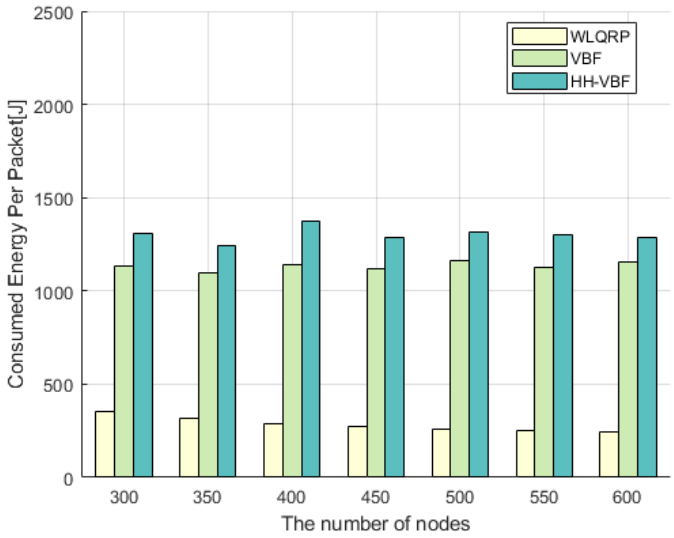

Figure 11. Consumed energy per packet.

5.3.6. Deviation Factor

Figure 12 presents the evolving trends in the path deviation factor for the two protocols as the number of nodes increases. The path deviation factor is defined as the ratio of the discrepancy between the actual transmission distance of a data packet from source to sink and the theoretical straight-line distance to the theoretical straight-line distance between the source and sink nodes. Consequently, when the actual transmission distance of a data packet closely approximates the true distance, the path deviation factor is minimized, leading to reduced supplementary overhead.

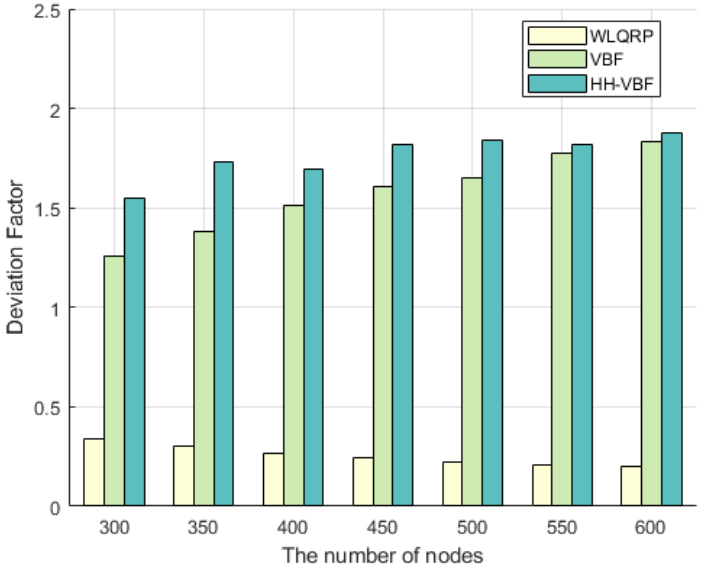

Figure 12. Deviation factor.

As observed from Figure 12 an augmentation in node count yields a lower path deviation factor for WLQRP, signifying a closer alignment with the actual path and diminished supplementary overhead. In contrast, the path deviation rate of VBF and HH-VBF rise as the number of nodes increases. This phenomenon arises from the higher likelihood of nodes aligning with the straight-line path between the source and sink nodes as the node count escalates. When selecting relays, WLQRP comprehensively considers the link quality of both next-hop and subsequent nodes, enabling it to opt for the most suitable relay based on factors such as position, success rate, and energy, effectively reducing supplementary overhead. Conversely, the increased node count under VBF and HH-VBF introduces interference in selecting the optimal relay, resulting in an elevated path deviation factor.

6. Conclusions

Taking into account the distinctive features of communication underwater using acoustic signals, the design of routing protocols must address factors such as the properties of signal propagation in water, the limited energy capacity of sensor nodes, and the ever-changing network topology. In order to improve the dependability of sensor networks and decrease energy usage, this research paper suggests a routing protocol called WLQRP that is both reliable and energy-efficient. WLQRP not only effectively bypasses node void areas by considering the link quality to the next hop and the next-to-next hop nodes, thus improving communication reliability, but also reduces energy consumption by pre-determining the optimal relay node through handshake messages, reducing redundant transmissions. The experimental simulation findings indicate that WLQRP improves network performance by increasing the data transmission rate, reducing energy consumption, and decreasing end-to-end latency. This implies that WLQRP is effective in minimizing network energy usage and enhancing network reliability. Unlike other protocols that sacrifice latency for other performance metrics, WLQRP maintains lower latency while achieving superior

performance in these metrics compared to the VBF protocol. For future work, we will focus on researching how to adaptively adjust the weight coefficients for link quality based on the network's channel conditions and topology, thus enhancing the performance of the routing algorithm.

Author Contributions: Conceptualization, J.W.; methodology, J.W. and H.Y.; software, J.W.; validation, J.W.; formal analysis, J.W.; investigation, J.W.; resources, J.Y.; data curation, J.W.; writing—original draft preparation, J.W., Y.G. and Z.W.; writing—review and editing, J.W., J.Y., Z.P. and H.Y.; visualization, J.W.; supervision, J.Y. and H.Y.; project administration, J.Y. and H.Y.; funding acquisition, J.Y. and H.Y. All authors have read and agreed to the published version of the manuscript.

Funding: This research was funded by the National Natural Science Foundation of China (grant number: U22A2012); the National Natural Science Foundation of China (grant number: 72064007); and the Research Initiation Fund of Guilin University of Technology (grant number: GUTQDJJ2017).

Data Availability Statement: The data presented in this paper are available after contacting the corresponding author.

Conflicts of Interest: The authors declare no conflict of interest.

References

1. Sandeep, D.N.; Kumar, V. Review on Clustering, Coverage, and Connectivity in Underwater Wireless Sensor Networks: A Communication Techniques Perspective. *IEEE Access* **2017**, *5*, 11176–11199. [CrossRef]
2. Sozer, E.M.; Stojanovic, M.; Proakis, J.G. Underwater Acoustic Networks. *IEEE J. Ocean. Eng.* **2000**, *25*, 72–83. [CrossRef]
3. Pompili, D.; Akyildiz, I.F. Overview of Networking Protocols for Underwater Wireless Communications. *IEEE Commun. Mag.* **2009**, *47*, 97–102. [CrossRef]
4. Melodia, T.; Kulhandjian, H.; Kuo, L.-C.; Demirors, E. Advances in Underwater Acoustic Networking. In *Mobile Ad Hoc Networking: Cutting Edge Directions*, 2nd ed.; Chapter 23; Basagni, S., Conti, M., Giordano, S., Stojmenovic, I., Eds.; Wiley: New York, NY, USA, 2013; pp. 804–852.
5. Ghoreyshi, S.M.; Shahrabi, A.; Boutaleb, T. Void-Handling Techniques for Routing Protocols in Underwater Sensor Networks: Survey and Challenges. *IEEE Commun. Surv. Tutorials* **2017**, *19*, 800–827. [CrossRef]
6. Jianmin, Y.; Gang, Q.; Songzuo, L.I.U.; Yanling, Y.I.N. A Medium Access Control Protocol for Underwater Acoustic Communication Networks with Directional Antennas. *Acta Acustica.* **2020**, *45*, 675–682.
7. Gang, Q.; Liu, S.-Z.; Liu, Q.-P. Review of Protocols, Simulation, and Experimentation for Underwater Acoustic Communication Network. *IEEE Trans. Mob. Comput.* **2017**, *25*, 151–160. [CrossRef]
8. Zhang, X.; Cao, X.; Yan, L.; Sung, D.K. A Street-Centric Opportunistic Routing Protocol Based on Link Correlation for Urban VANETs. *IEEE Trans. Mob. Comput.* **2016**, *15*, 1586–1599. [CrossRef]
9. Climent, S.; Sanchez, A.; Capella, J. Underwater Acoustic Wireless Sensor Networks Advances and Future Trends in Physical, MAC and Routing Layers. *Sensors* **2014**, *14*, 795–833. [CrossRef]
10. Xie, P.; Cui, J.-H.; Lao, L. VBF: Vector-based forwarding protocol for underwater sensor networks. In *NETWORKING 2006. Networking Technologies, Services, and Protocols; Performance of Computer and Communication Networks; Mobile and Wireless Communications Systems*; Springer: Berlin, Heidelberg, 2006; Volume 3976, pp. 1216–1221.
11. Nicolaou, N.; See, A.; Xie, P.; Cui, J.; Maggiorini, D. Improving the robustness of location-based routing for underwater sensor networks. In Proceedings of the IEEE OCEANS 2007, Europe, Aberdeen, UK, 18–21 June 2007; pp. 1–6.
12. Yu, H.; Yao, N.; Liu, J. An adaptive routing protocol in underwater sparse acoustic sensor networks. *Ad Hoc Netw.* **2015**, *34*, 121–143. [CrossRef]
13. Kang, Y.; Su, Y.; Xu, Y. ACGSOR: Adaptive cooperation-based geographic segmented opportunistic routing for underwater acoustic sensor networks. *Ad Hoc Netw.* **2023**, *145*, 103158. [CrossRef]
14. Li, X.; Xu, S.; Zhao, H.; Han, S.; Yan, L. An adaptive multi-zone geographic routing protocol for underwater acoustic sensor networks. *Wirel. Netw.* **2022**, *28*, 209–223. [CrossRef]
15. Jiang, J.; Han, G.; Guo, H.; Shu, L.; Rodrigues, J.J.P.C. Geographic multipath routing based on geospatial division in duty-cycled underwater wireless sensor networks. *J. Netw. Comput. Appl.* **2016**, *59*, 4–13. [CrossRef]
16. Hwang, D.; Dongkyun, K. DFR: Directional flooding-based routing protocol for underwater sensor networks. In Proceedings of the OCEANS 2008, Quebec City, QC, Canada, 15–18 September 2008.
17. Ali, T.; Low, T.J.; Sadia, A. Flooding control by using angle-based cone for UWSNs. In Proceedings of the 2012 International Symposium on Telecommunication Technologies, Kuala Lumpur, Malaysia, 26–28 November 2012; pp. 112–117.
18. Guan, Q.; Ji, F.; Liu, Y.; Yu, H.; Chen, W. Distance-Vector-Based Opportunistic Routing for Underwater Acoustic Sensor Networks. *IEEE Internet Things J.* **2019**, *6*, 3831–3839. [CrossRef]
19. Yan, H.; Shi, Z.J.; Cui, J.H. DBR: Depth-based routing for underwater sensor networks. In Proceedings of the 7th International IFIP-TC6 Networking Conference Singapore, Berlin/Heidelberg, Germany, 5–9 May 2008; pp. 72–86.

20. Mohammadi, R.; Javidan, R.; Jalili, A. Fuzzy depth based routing protocol for underwater acoustic wireless sensor networks. *J. Telecommun. Electron. Comput. Eng.* **2015**, *7*, 81–86.
21. Yu, H.; Yao, N.; Wang, T.; Li, G.; Gao, Z.; Tan, G. WDFAD-DBR: Weighting depth and forwarding area division DBR routing protocol for UASNs. *Ad Hoc Netw.* **2016**, *37*, 256–282. [CrossRef]
22. Noh, Y.; Lee, U.; Wang, P.; Choi, B.S.C.; Gerla, M. VAPR: Void-aware pressure routing for underwater sensor networks. *IEEE Trans. Mob. Comput.* **2013**, *12*, 895–908. [CrossRef]
23. Wahid, A.; Dongkyun, K. An energy efficient localization-free routing protocol for underwater wireless sensor networks. *Int. J. Distrib. Sens. Netw.* **2012**, *2012*, 307246. [CrossRef]
24. Noh, Y.; Lee, U.; Lee, S. HydroCast: Pressure Routing for Underwater Sensor Networks. *IEEE Trans. Veh. Technol.* **2016**, *65*, 333–347. [CrossRef]
25. Ashraf, S.; Gao, M.; Chen, Z.; Naeem, H.; Ahmed, T. CED-OR Based Opportunistic Routing Mechanism for Underwater Wireless Sensor Networks. *Wirel. Pers. Commun.* **2022**, *125*, 487–511. [CrossRef]
26. Karim, S.; Shaikh, F.K.; Chowdhry, B.S.; Mehmood, Z.; Tariq, U.; Naqvi, R.A.; Ahmed, A. GCORP: Geographic and Cooperative Opportunistic Routing Protocol for Underwater Sensor Networks. *IEEE Access* **2021**, *9*, 27650–27660. [CrossRef]
27. Bouk, S.H.; Ahmed, S.H.; Park, K.-J.; Eun, Y. EDOVE: Energy and Depth Variance-Based Opportunistic Void Avoidance Scheme for Underwater Acoustic Sensor Networks. *Sensors* **2017**, *17*, 2212. [CrossRef] [PubMed]
28. Ayaz, M.; Abdullah, A. Hop-by-hop dynamic addressing based (H2-DAB) routing protocol for underwater wireless sensor networks. In Proceedings of the 2009 International Conference on Information and Multimedia Technology, Jeju Island, Republic of Korea, 16–18 December 2009.
29. Zhang, W.; Wang, J.; Han, G.; Feng, Y.; Tan, X. A Nonuniform Clustering Routing Algorithm Based on a Virtual Gravitational Potential Field in Underwater Acoustic Sensor Network. *IEEE Internet Things J.* **2023**, *10*, 13814–13825. [CrossRef]
30. Wang, K.; Gao, H.; Xu, X.; Jiang, J.; Yue, D. An Energy-Efficient Reliable Data Transmission Scheme for Complex Environmental Monitoring in Underwater Acoustic Sensor Networks. *IEEE Sens. J.* **2016**, *16*, 4051–4062. [CrossRef]
31. Wan, Z.; Liu, S.; Ni, W.; Xu, Z. An energy-efficient multi-level adaptive clustering routing algorithm for underwater wireless sensor networks. *Clust. Comput.* **2019**, *22*, 14651–14660. [CrossRef]
32. Khan, W.; Wang, H.; Anwar, M.S.; Ayaz, M.; Ahmad, S.; Ullah, I. A Multi-Layer Cluster Based Energy Efficient Routing Scheme for UWSNs. *IEEE Access* **2019**, *7*, 77398–77410. [CrossRef]
33. Basagni, S.; Petrioli, C.; Petroccia, R.; Spaccini, D. CARP: A Channel-aware routing protocol for underwater acoustic wireless networks. *Ad Hoc Netw.* **2014**, *7*, 29. [CrossRef]
34. Zhou, Z.; Yao, B.; Xing, R.; Shu, L.; Bu, S. E-CARP: An Energy Efficient Routing Protocol for UWSNs in the Internet of Underwater Things. *IEEE Sens. J.* **2016**, *16*, 4072–4082. [CrossRef]
35. Domingo, M.C.; Prior, R. Energy analysis of routing protocols for underwater wireless sensor networks. *Comput. Commun.* **2008**, *31*, 1227–1238. [CrossRef]
36. Stojanovic, M. On the relationship between capacity and distance in an underwater acoustic channel. In Proceedings of the First ACM International Workshop on Underwater Networks (WUWNeT'06), Los Angeles, CA, USA, 25 September 2006; pp. 41–47.
37. Zhao, L.; Liang, Q. Optimum cluster size for underwater acoustic sensor networks. In Proceedings of the Military Communications Conference, Washington, DC, USA, 23–25 October 2006.
38. Mackenzie, K.V. The nine-term equation for sound speed in the oceans. *J. Acoust. Soc. Am.* **1981**, *70*, 807–812. [CrossRef]